Deep structures of the Ecuador convergent margin and the Carnegie Ridge, possible consequence on great earthquakes recurrence interval

David Graindorge,[1] Alcinoe Calahorrano,[1,2,3] Philippe Charvis,[3] Jean-Yves Collot,[3] and Nicole Bethoux[4]

Received 9 October 2003; accepted 15 December 2003; published 17 February 2004.

[1] The deep structure of the Ecuador subduction zone and adjacent Carnegie Ridge (CR) was investigated using on-shore off-shore wide-angle seimics. A crustal model obtained by 2-D inversion of traveltimes reveals the overthickened (14 km) oceanic crust of the CR that underthrusts the high velocity (>6 km/s) basement of the upper plate margin wedge, interpreted as part of the accreted oceanic terranes described on-shore. The plate interface dips 4° to 10° east from the trench to a depth of 15 km. Shadow zones observed on the margin OBS records are interpreted as a low velocity zone consisting of a thin layer of underthrust sediments, and the 3-km-thick CR layer 2, whose average seismic velocity of 5.1 km/s is slower than that of the margin wedge. Increased interplate coupling related to the subduction of the thick, buoyant CR may account for an apparent local increased recurrence interval between great interplate earthquakes. *INDEX TERMS:* 3025 Marine Geology and Geophysics: Marine seismics (0935); 7230 Seismology: Seismicity and seismotectonics; 8015 Structural Geology: Local crustal structure; 8105 Tectonophysics: Continental margins and sedimentary basins (1212); 8150 Tectonophysics: Plate boundary—general (3040). **Citation:** Graindorge, D., A. Calahorrano, P. Charvis, J.-Y. Collot, and N. Bethoux (2004), Deep structures of the Ecuador convergent margin and the Carnegie Ridge, possible consequence on great earthquakes recurrence interval, *Geophys. Res. Lett.*, *31*, L04603, doi:10.1029/2003GL018803.

1. Introduction

[2] Great subduction earthquakes depend on various parameters including the nature and structure of both the downgoing crust and overlying margin. Attention has been drawn to the subduction of large oceanic seamounts in coupled margins, which likely increases the normal stress across the plate interface and therefore enhances the plate coupling. Such a process can lead to an increase in the recurrence intervals of earthquakes [*Scholz and Small*, 1997]. Voluminous and compensated subducting ridges may have similar effects. At the Ecuador trench, between 0.5°N–2.2°S (Figure 1), the CR, an overthickened massive, 300-km wide oceanic plateau rising 1500 m above surrounding sea-floor [*Bentley*, 1974] and resulting from the Neogene interaction between the Galapagos hotspot and the Cocos-Nazca spreading center [*Lonsdale*, 1978], underthrusts the volcano-oceanic accreted terranes (known as Piñon formation) [*Hughes and Pilatasing*, 2002] of the Ecuadorian margin. At these latitudes, a 5.4 ± 0.2 cm/yr eastward convergence between the Nazca and South America plates is responsible for accumulation of significant elastic strain across the margin [*Trenkamp et al.*, 2002]. During the last century, the CR subduction has been associated with a sequence of five great earthquakes ($7.7 < M < 8.8$), which occurred between Guayaquil and Tumaco [*Kanamori and McNally*, 1982; *Gutscher et al.*, 1999] (Figure 1). Based on these observations, we consider that the Ecuador margin is partially coupled.

[3] The purpose of this paper is to use wide-angle seismic data to investigate (1) the crustal velocity structure of the CR and the Ecuador margin wedge, (2) the shape and nature of the plate interface at depths, and (3) finally to discuss a possible relationship between the subduction of the CR crustal structure and the recurrence interval of great subduction earthquakes.

2. Data and Analysis Method

[4] During the SISTEUR experiment [*Collot et al.*, 2002], we deployed 11 OBS and land stations along a transect at 1.4°S where an airgun array of 128 l (7814 in^3) was fired each 125 m (Figure 1). Phases observed on records are described in Figure 2.

[5] The velocity model was developed through a combination of traveltime inversion and amplitude modeling of observed arrivals. Forward ray-trace modeling was first applied to get a starting model. Then travel times of refractions and reflections phases were then inverted using the raytrace-based inversion scheme of *Zelt and Smith* [1992].

3. Velocity Structure

3.1. Model Uncertainty

[6] We assessed the quality of the final velocity model using the fit between predicted and observed travel times and the resolution of velocity and interface nodes related to the ray coverage (Figure 3, Table 1). The nodes with a resolution value >0.5 are considered to be well resolved [*Zelt and Smith*, 1992]. RMS misfits for individual layers range from 0.05 to 0.22 s, comparable to phase pick errors (0.04 to 0.15 s) (Table 1). For amplitude modeling, synthetic seismograms were calculated using zero-order asymp-

[1]UMR Géosciences Azur, Université Pierre et Marie Curie, Observatoire Océanologique de Villefranche, Villefranche-sur-mer, France.
[2]Escuela Politecnica Nacional, Ladrón de Guevara, Quito, Ecuador.
[3]UMR Géosciences Azur, Institut de Recherche pour le Développement, Villefranche-sur-mer, France.
[4]UMR Géosciences Azur, Université de Nice Sophia Antipolis, Villefranche-sur-mer, France.

0094-8276/04/2003GL018803

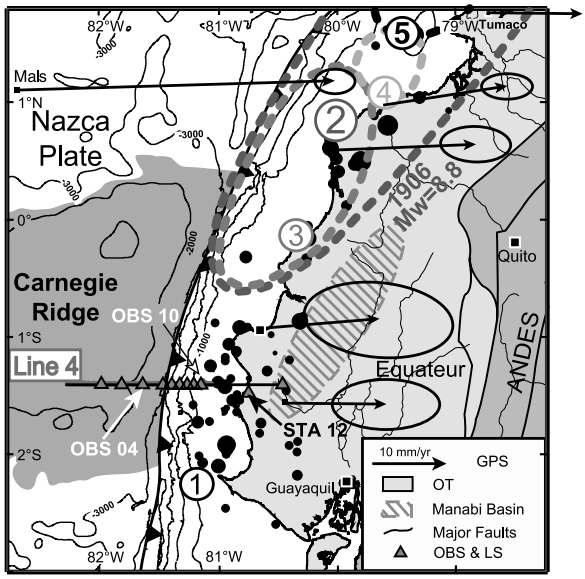

Figure 1. Geodynamic setting of the Ecuadorian subduction zone. Circles indicate Mb > 4 earthquakes relocated by *Engdahl et al.* [1998] scaled by magnitude. Numbered circles indicate the five last century largest earthquakes (M > = 7.7: (1) 1901, (2) 1906, (3) 1942, (4) 1958, (5) 1979, [*Kanamori and McNally*, 1982; *Swenson and Beck*, 1996]. Black arrows indicate observed GPS vectors relative to South America from *Trenkamp et al.* [2002]. Mals vector corresponding to observed GPS vector, on Malpelo Island, has been displaced to fit in the frame. Carnegie Ridge is defined by the 2500 m depth contour (dark gray). Triangles show locations of OBS and land-seismometers (LS) and the plain line the shooting line for profile 4 used in this study. OT stand for "oceanic terranes accreted in the early tertiary".

totic ray theory [*Cerveny et al.*, 1977]. The resulting synthetic seismograms fit the general trends of critical point locations and provides an acceptable fit to the data (Figure 2c) particularly for the shadow zone.

3.2. Carnegie Ridge Crustal Structure

[7] The CR has a three-velocity-layer oceanic structure. Layer 1 with a thickness of 0.2 to 0.9 km and velocities ranging from 2.4 km/s at the top to 2.8 km/s at the base, has been drilled 300 km west of the trench at DSDP site 157 [*van Andel*, 1973]. Cores recovered at this site revealed 431 m of Neogene and Quaternary sediments with sonic velocity reaching 2.5 km/s overlying Neogene basalts with mean sonic velocity of 4.5 km/s [*van Andel*, 1973]. Layer 2 with a thickness of 2.8 km and mean velocities of 4.8 km/s at the top and 5.5 km/s at the base, comparable to those of oceanic layer 2b, is well resolved in the central part of our model (Figure 3). The 10.5-km-thick layer 3 velocities ranging from 6.4 km/s at its top to 7.3 km/s at its base fit well with typical oceanic layer 3 [*White et al.*, 1992]. On CR the layer 2/layer 3 thickness ratio [*Mutter and Mutter*, 1993] is 0.28 (0.6 for normal oceanic crusts). For oceanic plateaus emplaced in the vicinity of a hotspot, crustal thickening is dominated by layer 3 [e.g., 0.27 for the Kerguelen Plateau; *Charvis et al.*, 1995]. The 14 km-thick CR seismic structure is consistent with the oceanic plateau origin proposed by *Lonsdale* [1978] and more recently by *Sallarès et al.* [2002].

3.3. Upper Plate Structure

[8] Modeling of wide-angle data across the Ecuadorian margin leads to a three-layer upper plate crustal structure (Figure 4). Layer A with velocities ranging from 1.9 to 2.2 km/s and an average thickness of 0.8 km is interpreted as sedimentary rocks. Layer B with a velocity of ~3.8 km/s at its top, a velocity of ~5.1 km/s at its base and large lateral variations in thickness may correspond to Upper Cretaceous volcano-clastics known onshore [*Jaillard et al.*, 1997]. The Cenozoic Manabi Basin is likely to account for the delay

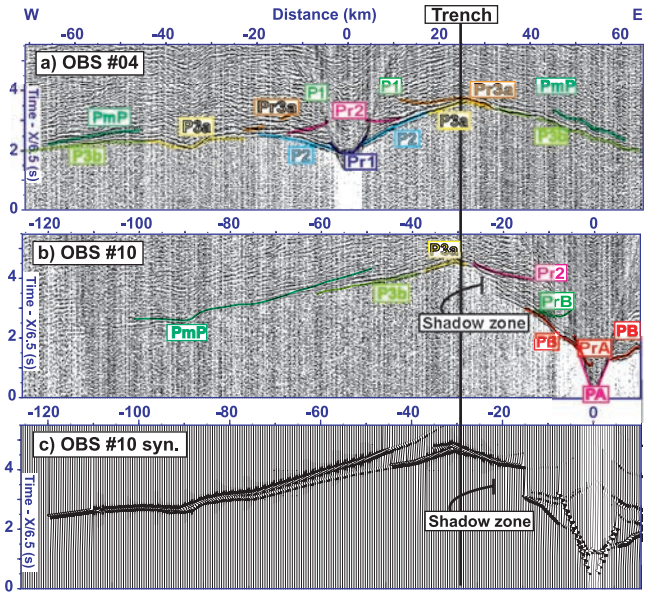

Figure 2. Wide-angle seismic record sections (vertical component) for OBS 04 (a) and OBS 10 (b) along line 4 (Figure 1). A band-pass filter between 5 and 20 Hz, a predictive deconvolution and an equalization of amplitudes were applied to the data before plotting with a reduction velocity of 6.5 km/s. Color lines outline calculated travel times. The different phases observed are labeled: 1) PmP reflection from oceanic Moho, 2) P3a and P3b, waves refracted within oceanic layer 3, 3) P2 wave refracted within oceanic layer 2 (only on OBS located on the CR), 4) P1 refracted within oceanic sediments (layer 1). Reflected phases are designated by Pr1, Pr2, Pr3, for reflections from the base of layers 1, 2, and 3. For OBS and land stations located on the upper plate, seismic records show additional phases at short offset: 1) PA refracted phase within shallow margin sediments, 2) PB phase corresponding to turning rays within a second crustal layer with higher seismic velocity (B), 3) PC refracted phase within a high velocity layer (C) overlying the lower plate (not shown). Reflected phases from the base of layers A and B have also been observed and modeled (PrA and PrB). Records from seismometers located on the margin show a shadow zone which increases landward from 0.3 s to 1.1 s. (c) For comparison a synthetic seismogram of seismic section recorded by OBS 10 is calculated from the final crustal model with comparable plotting parameters.

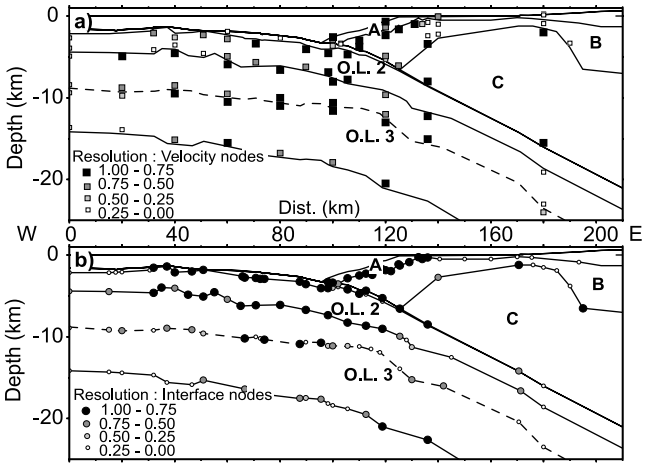

Figure 3. Resolution values calculated from the travel time inversion of the final velocity model: resolution values of the velocity nodes (a), and resolution values of the interface nodes (b).

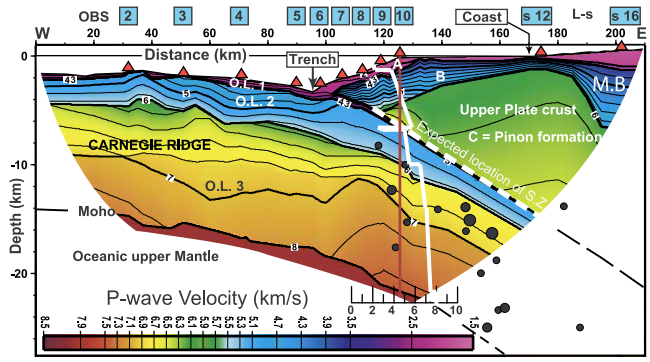

Figure 4. Final velocity model across the Ecuadorian margin. Color-coded velocities are plotted for part of the model sampled by rays. Black circles indicate position of earthquakes from Engdhal's catalogues projected over a distance of 50 km on each side of the profile. Manabi Basin: M.B., inferred seismogenic zone: S.Z., and oceanic layer: O.L., Land-stations: L-s. 1D velocity model at 125.40 km (OBS 10) is plotted on the 2D model.

required for modeling of land station 16 arrivals traveling within layer C.

[9] Laboratory measurements indicate that the seismic velocity of a basalt and a zeolite facies basalt at 200 Mpa (depth ~7 km) are respectively 6.00 km/s and 6.30 km/s [*Christensen*, 1996]. Layer C velocities ranging from 6.1 to 6.4 km/s (Figure 4) are consistent with the oceanic rocks of the Piñon formation outcropping on land [*Baldock*, 1983]. In a similar geological context, velocities comparable or lower than those of layer C have been interpreted as oceanic basement in the margin wedge of Costa-Rica [*Ye et al.*, 1996].

3.4. Plate Interface and Low Velocity Zone

[10] Wide-angle data modeling provides constraints on the plate boundary between 4 and 15 km depths. The subducting plate dips 4° beneath the margin slope and 10° beneath the shelf and the coast (Figures 3a–3b) at 1.4°S. The shadow zone observed on the OBS record sections (Figure 2a) between waves refracted in the upper plate (PB or PC, Figure 2b) and those refracted in the lower plate (P3a, Figure 2b), can be interpreted as a low velocity zone. Other low velocity zones have been described at subduction plate interfaces. Although a clear shadow zone is not apparent in the OBS records from the NE Japan fore-arc, *Takahashi et al.* [2000] modeled the high amplitude of the waves reflected at the top of the subducting crust, by introducing a low velocity layer (LVL). The LVL consisted of a 4 km/s, 100 m-thick sedimentary layer located between oceanic layer 2 and the island arc crust. In Costa Rica, a LVZ resulting from incoming sediments is interpreted from both high amplitude reflections and travel time delay between upper and lower plate refracted phases [*Ye et al.*, 1996]. High amplitude phases reflected from the top (e.g., phase PrB, Figure 2b) and from the base of the low-velocity zone (e.g., phase Pr3a, Figure 2) are observed in our data set. These high amplitude reflections are well modeled in the synthetic seismograms (Figure 2c). Coincident MCS data [*Collot et al.*, 2002] indicate that Nazca Plate sediments are thrust beneath the upper plate. However, this thin subducting sedimentary section, which extends beneath the inner trench slope, cannot account for the shadow zone as thick as 1.1 s observed on the OBS 10 (Figure 2b). Considering that the velocity of the CR layer 2 remains about constant (~5.1 km/s) beneath the Ecuador margin, a 3–4 km-thick LVZ can be estimated. The 1D velocity

Table 1. Observed Phases and Travel Time Fits for the Final Model (Figure 4)

Layer	Phase	Instruments	Pick Uncertainty,	Number of Travel Times	RMS Misfit, s
Layer A	PA	OBS 10	0,06	36	0,073
Layer A	PrA	OBS 6, 7, 10	0,15	99	0,275
Layer B	PB	OBS 7 to 10	0,05	266	0,059
Layer B	PrB	OBS 8 to 10	0,08	99	0,095
Layer C	PC	SI 12, 16	0,04	50	0,046
Layer 1	P1	OBS 4 to 6	0,15	17	0,224
Layer 1	Pr1	OBS 4, 5	0,09	27	0,092
Layer 2	P2	OBS 2 to 7	0,04	238	0,049
Layer 2	Pr2	OBS 2 to 7, 9, 10	0,1	298	0,158
Layer 3	P3	OBS 2 to 10, SI 12	0,05	432	0,069
Layer 3	Pr3	OBS 2 to 6, 8, SI 12	0,09	267	0,099
Layer 4	P4	OBS 2 to 6, 8 to 10, SI 12, SI 16	0,1	543	0,122
Layer 4	PmP	OBS 2 to 6, 8 to 10, SI 12	0,15	590	0,173

Pick uncertainties of arrivals were estimated depending on signal-to-noise ratios. RMS: Root-Mean-Square of the misfit between the calculated and observed travel times.

profile beneath the OBS 10 (Figure 4) reveals that the velocity of the CR oceanic layer 2 (5.1 km/s) is lower than the velocity of the deepest part of layer C (~6.0 km/s) accounting mainly for the observed shadow zone beneath the continental shelf (Figures 2 and 4).

4. Discussion

[11] Our data set show that the overthickened crust of the CR extends beneath the Ecuador margin at least up to the coast line, proving that CR has been subducting since at least 1.4 Ma, based on a 57 mm/yr convergence rate [*Trenkamp et al.*, 2002]. This minimum age agrees with other suggestions, and is close to the 1.8 Ma geodynamic estimation of *Lonsdale* [1978] and *Pennington* [1981].

[12] According to its history of great subduction earthquakes, the Ecuador margin in contact with CR can be divided in two segments. Immediately north of 0.5°S, the 1906 and 1942, earthquakes ruptured the plate boundary adjacent to the northern flank of CR, [*Kanamori and McNally*, 1982; *Mendoza and Dewey*, 1984; *Swenson and Beck*, 1996], whereas between 0.5°S and 2.2°S, the poorly defined 1901 event (Ms = 7.8, SISRA catalogue) occurred somewhere at the junction between the trench and the southern flank of CR [*Gutscher et al.*, 1999] (Figure 1). Therefore, the 0.5°S–2.2°S margin segment, where the bulk of the CR is subducting, has not been affected by a large earthquake for one century and possibly for a yet longer time in the case the 1901 earthquake was not an interplate event. In contrast, the 0.5°S–~0.5°N margin segment ruptured twice over the same time period (Figure 1). Although scarce, these observations suggest an apparent greater earthquake recurrence interval where the bulk of CR is subducting. *Scholz and Small's model* [1997] developed for subducting seamounts appears to be also valid for large and thick volcanic ridges, such as the CR. Recent GPS results show that elastic strain has been equally accumulating across both margin segments (Figure 1), indicating that the plate interface is partially locked in this area [*Trenkamp et al.*, 2002]. However, along the southern segment, the plate interface, and therefore the locked zone, is longer (~180 km) than along the northern one (~100 km). Consequently, we suggest that stronger normal stress related to the CR buoyancy, together with a larger CR surface involved in the subduction locked zone between 0.5°S and 2.2°S would locally enhance the mechanical coupling between the plates and would therefore be responsible for the observed increase in the recurrence interval of large earthquakes.

5. Conclusion

[13] Analysis and modeling of wide angle seismic data collected along a transect of the CR and the Ecuador margin at 1.4°S provide original results. (1) The CR is a three-layer overthickened oceanic crust, which reaches 14 km in thickness beneath its southern flank. The main contribution of overthickening is due to oceanic layer 3 (lower crust), and layer 2/layer 3 ratio is 0.28, both results being consistent with an oceanic plateau origin. (2) The CR has been subducting since at least 1.4 Ma. (3) The basement and deep crust of the offshore Ecuador margin is characterized by P-wave velocities ranging from 3.7 to 6.3 km/s, which are consistent with the oceanic nature of basement outcropping onshore. (4) The subducting slab dips 10° east between 4–15 km depth. (5) The delays in first arrival travel times suggest a low velocity zone in the vicinity of the plate boundary. The primary contributor is likely oceanic layer 2 of the subducted CR (~5.1 km/s), thrust beneath the 6 km/s margin wedge, with possible additional contribution from subducted sediments. (6) The apparent increase recurrence time of major subduction earthquakes observed in the study area with respect to northern flank of CR may be driven by a local increase of the mechanical plate coupling due to the subduction of the thick, buoyant CR.

[14] **Acknowledgments.** We thank the SISTEUR scientific party, technical staff, captains, officers, and crews of R/V Nadir (IFREMER) and Orion (INOCAR). We acknowledge Yann Hello and Alain Anglade for operating the OBS, and reviewers for constructive remarks. This project was funded by IFREMER, Institut de Recherche pour le Développement, Institut National des Sciences de l'Univers, Université Pierre et Marie Curie, the French Embassies in Colombia and Ecuador, the Departamanto de Geofisica of the Escuela Politecnica Nacional de Quito, and the European Community Program "Improving Human Potential: Access to large Scale Facilities". This is Géosciences Azur contribution number 604.

References

Baldock, J. W. (1983), The Northern Andes: A review of the Ecuadorian Pacific Margin, in *The Oceans Basins and Margins*, edited by A. E. M. Nairn, F. G. Stehli, and S. Uyeda, Plenum Press, New-York and London, 181–271.

Bentley, L. R. (1974), Crustal structure of the Carnegie ridge, Panama basin and Cocos ridge, Master's thesis, Hawaii.

Cerveny, V., I. Molotkov, and I. Psencik (1977), Ray Method in Seismology, Charles Univ. Press, Prague, Czechoslovakia.

Charvis, P., M. Recq, S. Operto, and D. Bréfort (1995), Deep structure of the Kerguelen-Heard Plateau and hot spot-related activity, *Geophys. J. Int.*, *122*, 899–924.

Christensen, N. I. (1996), Poisson's ratio and crustal seismology, *J. Geophys. Res.*, *101*(B2), 3139–3156.

Collot, J. Y., P. Charvis, M. A. Gutscher, and S. Operto (2002), Exploring the Ecuador-Colombia active margin and interplate seismogenic zone, *EOS Trans., AGU*, *83*(17), 189–190.

Engdahl, E. R., R. P. Van der Hilst, and R. P. Buland (1998), Global teleseismic earthquake relocation with improved travel times and procedures for depth determination, *Bull. Seismol. Soc. Am.*, *88*, 722–743.

Gutscher, M. A., J. Malavieille, S. E. Lallemand, and J. Y. Collot (1999), Tectonic segmentation of the North Andean margin: Impact of the Carnegie Ridge collision, *Earth Planet. Sci. Lett.*, *168*, 255–270, 1999.

Hughes, R. A., and L. F. Pilatasing (2002), Cretaceous and Tertiary terrane accretion in the Cordillera Occidental of the Andes of Ecuador, *Tectonophysics*, *345*(1–4), 29–48.

Jaillard, E., S. Benitez, and G. H. Mascle (1997), Les déformations paléogènes de la zone d'avant-arc sud-équatorienne en relation avec l'évolution géodynamique, *Bull. Soc. Géol. France*, *168*, 403–412.

Kanamori, H., and K. C. McNally (1982), Variable rupture mode of the subduction zone along the Ecuador-Colombia coast, *Bull. Seismol. Soc. Am.*, *72*, 1241–1253.

Lonsdale, P. (1978), Ecuadorian Subduction System, *Am. Ass. Petrol. Geol. Bull.*, *62*(12), 2454–2477.

Mendoza, C., and J. W. Dewey (1984), Seismicity associated with the great Colombia-Ecuador earthquakes of 1642, 1958 and 1979: Implications for barrier models of earthquake rupture, *Bull. Seismol. Soc. Am.*, *74*, 577–593.

Mutter, C. Z., and J. C. Mutter (1993), Variations in thickness of layer 3 dominate oceanic crustal structure, *Earth Planet. Sci. Lett.*, *117*, 295–317.

Pennington, W. D. (1981), Subduction of the eastern Panama basin and seismotectonics of northwestern South America, *J. Geophys. Res.*, *86*, 10,753–10,770.

Sallarès, V., P. Charvis, E. R. Flueh, J. Bialas, and C. Walther (2002), Wide-angle seismic constraints on the evolution of Galapagos hotspot—Cocos-Nazca spreading center interaction, *EGS XXVII General Assembly*, Abstr. EGS02-A-03145.

Scholz, C. H., and C. Small (1997), The effect of seamount subduction on seismic coupling, *Geology*, *25*(6), 487–490.

Swenson, J. L., and S. L. Beck (1996), Historical 1942 Ecuador and 1942 Peru Subduction Earthquakes, and Earthquakes Cycles along Colombia-Ecuador and Peru Subduction Segments, *Pure Appl. Geophys.*, *146*(1), 67–101.

Takahashi, N., S. Kodaira, T. Tsuru, J. Park, and Y. Kaneda (2000), Detailed plate boundary structure of northeast Japan coast, *Geophys. Res. Lett.*, *27*(13), 1977–1980.

Trenkamp, R., J. N. Kellogg, J. T. Freymueller, and P. Hector Mora (2002), Wide plate margin deformation, southern Central America and northwestern South America, CASA GPS observations, *J. Sou. Am. Sci.*, *15*(2), 157–171.

van Andel, T. H. (1973), Site 157, in *Initial reports of the Deep Sea Drilling Project*, edited by U. S. G. P. Office, pp. 53–150, U. S. Govt. Printing Office, Washington, D. C.

White, R. S., D. McKenzie, and R. K. O'Nions (1992), Oceanic Crustal Thickness From Seismic Measurements and Rare Earth Element Inversions, *J. Geophys. Res.*, *97*(B13), 19,683–19,715.

Ye, S., J. Bialas, E. R. Flueh, A. Stavenhagen, R. von Huene, G. Leandro, and K. Hinz (1996), Crustal structure of the Middle American Trench off Costa Rica from wide-angle seismic data, *Tectonics*, *15*(5), 1006–1021.

Zelt, C. A., and R. B. Smith (1992), Seismic traveltime inversion for 2-D crustal velocity structure, *Geophys. J. Int.*, *108*, 16–34.

N. Bethoux, A. Calahorrano, P. Charvis, J.-Y. Collot, and D. Graindorge, UMR Géosciences Azur, 06235, Villefranche-sur-mer, France. (david.graindorge@obs-vlfr.fr)